第33卷 第9期 焊 接 学 报 Vol. 33 No. 9
2012年9月 TRANSACTIONS OF THE CHINA WELDING INSTITUTION September 2012

铜钢异种材料等离子弧焊接头性能

程东海， 邵景辉， 陈益平， 胡德安
(南昌航空大学 航空制造工程学院，南昌 330063)

程东海

摘 要：采用LHM-200等离子弧焊机对1 mm紫铜与低碳钢异种材料进行了熔透型等离子弧焊试验，得到了内部无缺陷、外观成形良好的接头. 观察了接头的显微组织，并分析了工艺参数对接头力学性能的影响. 结果表明，焊缝区中心显微组织呈细胞群状，界面两侧的组织特征呈现显著的不同，焊缝与铜侧界面没有明显的熔合线，局部呈漩涡状，钢侧与焊缝连接处出现了明显的分界线；最佳工艺为焊接电流为65 A，焊接速度为0.4 cm/s，离子气流量为0.7 L/min，此时接头抗拉强度可达176 MPa，试样断裂于铜母材热影响区.

关键词：铜钢异种材料；等离子弧焊；接头性能
中图分类号：TG442 **文献标识码**：A **文章编号**：0253－360X(2012)09－0097－04

0 序 言

紫铜具有优良的导电性和导热性，然而单一的铜及其合金在很多情况下都难以满足实际的工程要求[1]，现代焊接技术的发展已经可以将不同性能的材料焊接成复合零部件，既能满足各种性能要求，又可节约各种贵重材料，降低成本. 铜/钢焊接结构广泛应用于冶金(氧气枪喷嘴、高压氧气管道阻火器、复合钢板)、机电(电机转子短路环)、食品机械、酿酒(啤酒生产用糊化锅)、航空航天等工业部门，具有良好推广应用前景[2]. 如何实现铜钢异种材料的高质量和高可靠性的焊接工艺，一直是人们关注和研究的主要问题，目前对铜/钢异种材料焊接的研究主要集中在激光焊、钎焊、搅拌摩擦焊等焊接方法上[3-6]，对铜/钢异种材料的等离子弧焊的研究很少. 文中采用LHM-200等离子弧焊机对铜/钢异种材料进行了熔透型等离子弧焊的试验研究，通过合理设计焊接工艺以实现紫铜/低碳钢的等离子弧焊接.

1 试验方法

试验所用材料为1 mm厚T2紫铜和Q235钢，材料尺寸为60 mm×30 mm，主要物理性能见表1. 试验使用的等离子弧焊设备为上海金通电子设备有限公司LHM-200式等离子弧焊机，最大输出功率为7.4 kW，焊接电流为5～200 A，配合水冷式等离子弧焊枪. 室温拉伸试验试样形状尺寸如图1所示，焊缝位于试样的中心. 拉伸试验在WDW-100试验机上进行，最大载荷100 kN，加载速率1 mm/s.

收稿日期：2011－07－08

表1 材料的主要物理性能

Table 1 Physical properties of materials

材料	熔点 T/℃	热导率 λ/(m·K^{-1})	线膨胀系数 α_l/10^{-6}·K^{-1}	抗拉强度 R_m/MPa
T2紫铜	1 083	390	16.50	215～255
Q235钢	1 500	77.5	11.76	375～460

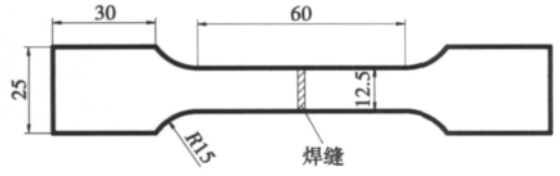

图1 拉伸试样尺寸示意图(mm)

Fig. 1 Sketch map of tensile specimen

2 试验结果及分析

2.1 焊接工艺对力学性能的影响

为了获得良好的铜钢异种材料等离子弧焊接头，通过设置3组工艺参数(焊接电流、焊接速度、离子气体流量)研究其对接头抗拉强度的影响.

2.1.1 焊接电流对抗拉强度的影响

图2为固定焊接速度0.4 cm/s、离子气体流量

0.7 L/min 时不同焊接电流下接头的抗拉强度. 从图 2 中可以看出,焊缝抗拉强度随着焊接电流的增加而增加.

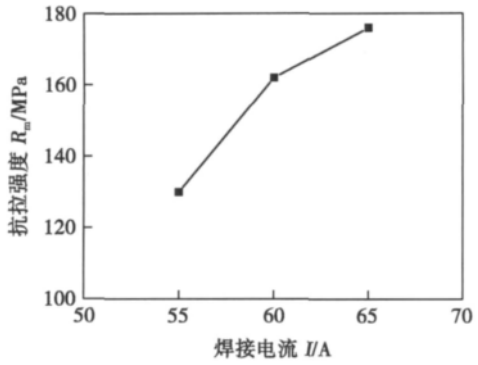

图 2 焊接电流对接头抗拉强度的影响

Fig. 2 Effects of current power on tensile strength of weld joint

在电流为 55 A 时抗拉强度仅为 130 MPa,由于电流较小,背面未充分熔透,正背面熔宽相差较多,符合熔透型等离子弧焊接焊缝断面呈碗状的特点. 随着焊接电流的增大,背面熔宽增加,抗拉强度显著提高,焊接电流为 65 A 时抗拉强度为 176 MPa,接近于铜母材的强度. 综上所述,焊接电流的提高有利于焊缝的背面熔透,实现单面焊双面成形,接头抗拉强度也有所提高.

2.1.2 焊接速度对抗拉强度的影响

图 3 为固定焊接电流 65 A、离子气体流量 0.7 L/min时不同焊接速度下接头的抗拉强度. 从图 3 中可以看出,焊缝抗拉强度随着焊接电流的增加而先突增后平稳. 在焊接速度为 0.3 cm/s 时,由于焊接速度较低,热输入较大,形成了过大的熔深而焊穿. 随着焊接速度的增加,热输入降低,焊缝的熔深随之减小,铜钢充分熔合而形成较好的焊缝. 当焊

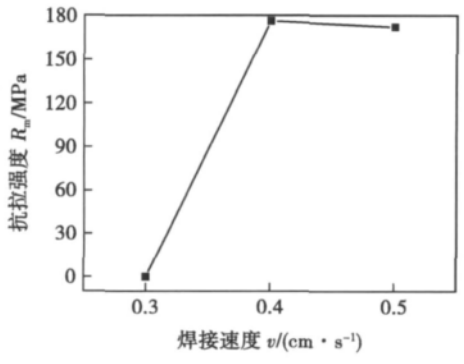

图 3 焊接速度对接头抗拉强度的影响

Fig. 3 Effects on weld speed on tensile strength of weld joint

接速度为 0.4 cm/s 时,接头抗拉强度达到最大值. 综上所述,焊接速度的提高,铜的熔化量逐渐减少,焊缝成形转好,接头抗拉强度逐渐提高.

2.1.3 离子气体流量对抗拉强度的影响

图 4 为固定焊接电流 65 A、焊接速度 0.4 cm/s 时不同离子气体流量下接头的抗拉强度. 从图 4 中可以看出,焊缝抗拉强度随着离子气体流量的增加而减小.

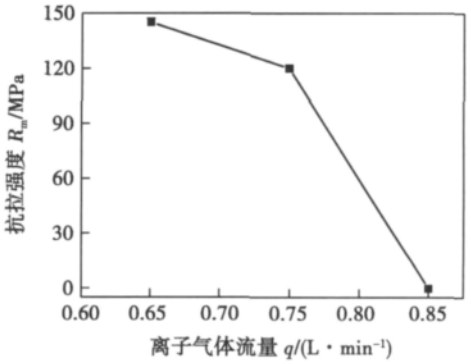

图 4 离子气体流量对接头抗拉强度的影响

Fig. 4 Effects of plasma flow on tensile strength of weld joint

在离子气体流量为 0.7 L/min 时,铜的熔化量最少,焊缝成形较好,热影响区软化程度最小,因此抗拉强度较高,达到 176 MPa. 随离子气体流量的增加,当离子气体流量为 0.9 L/min 时,铜的熔化量增加较快而使铜钢接头极易焊穿而不能形成焊接接头,说明接头抗拉强度对离子气体流量的变化较为敏感. 综上所述,离子气体流量的提高对焊缝成形不利,接头抗拉强度下降.

2.2 焊接接头显微组织

图 5a 为靠铜侧焊缝显微组织形貌,可以看到存在一个明显过渡带,在过渡带内大量块状组织弥散分布于铜侧母材基体上,说明铜侧的熔合情况较好,铜铁已经充分互溶形成不同于铜母材的过渡带块状组织.

图 5b 为靠钢侧焊缝显微组织形貌,可以看到存在明显的柱状晶区域,这是由于焊缝在冷却结晶过程中,由于等离子弧焊接速度较快,冷却过程中熔池形成了较大温度梯度和成分梯度造成的. 从图 5b 中还可以看出,钢侧与焊缝连接处出现了明显的分界线而不是如铜侧的过渡带块状组织,显然这是由于 Q235 低碳钢与 T2 紫铜物理、化学性能的差异而造成的.

图 5c 为焊缝区组织形貌,从焊缝区显微组织可

见,整个焊缝区域呈细胞群状,结合 Fe-Cu 二元合金相图分析可知,当铜含量小于 0.3% 时其组织为铜在铁中的固溶体 α 相; 当铁含量小于 0.2% 时形成铁在铜中的固溶体 ε 相; 当铜、铁含量在其它情况下形成双相组织,故焊缝区组织以($\alpha+\varepsilon$) 双相固溶体形式存在.

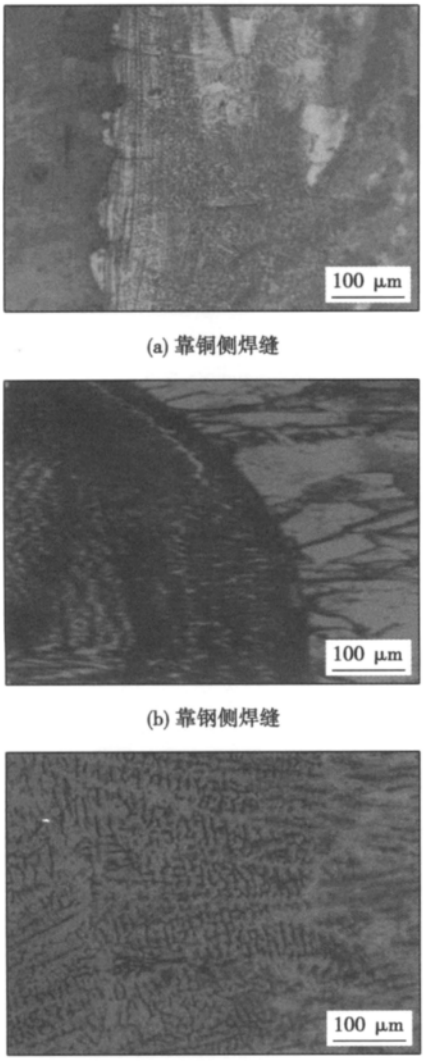

(a) 靠铜侧焊缝

(b) 靠钢侧焊缝

(c) 焊缝中心显微组织

图 5　焊接接头各区域显微组织形貌

Fig. 5　Microstructure of weld joint

通过对焊缝两侧典型界面组织特征进行分析,由于铜钢的热物理性能差异,在界面两侧形成了截然不同的组织,在铜侧界面形成了富铁带状组织以及弥散分布的颗粒相,在钢侧形成了铜钢互溶的圆形区域以及分布在其内部的颗粒相,之所以形成有别于同种金属焊接的界面,一方面由于焊接的加热冷却速度非常大,而且熔池的搅拌作用,促进了熔池中元素的对流以及热传导,另一方面和铜钢异种金属物理、力学性质有关,最重要的是焊接过程中熔池的温度梯度、热应力极不平衡.

综合以上因素分析认为铜钢异种金属等离子弧焊接的界面两侧差异主要包括以下几个原因. (1) 在焊接过程中,虽然钢的熔点高于铜,但是由于铜的热导率较大导致大量热量从侧面散失,钢热导率较低先熔化,而铜只有一定程度的少量熔化,铜和钢不同的冷却速率和凝固速度导致在快速凝固过程中独立的液相存在. 由于铜钢都处于液态下是无限互溶的,在熔池搅拌以及熔池的蒸气压力下,铜钢有一定程度的混合,但没有完全混合充分,因此界面局部形成了带状和球状的铜钢固溶体. (2) 由于热导率的关系,熔池中靠近钢侧界面存在的液态铜处于液态时间非常短,高熔点的铜首先发生凝固,在高强度的紊流及表面张力作用下在钢侧界面区域形成铜钢球互溶组织,而铜侧界面则形成了富铁的带状组织,其附近弥散分布着球状颗粒相. 从凝固界面形态稳定性原理出发的理论分析表明,熔体中因搅拌而产生的初生组织旋转运动有利于提高液—固界面稳定性,促进凝固核心保持球状稳定生长,从而有利于在焊接过程中获得球状组织. 研究表明剪切有利于球晶组织形成,且球晶组织有明显团聚现象. (3) 由铜—铁相图可知,铁在铜中的固溶量较小,因此钢基体中的铁熔化与熔池钢侧界面的液态铜有一定的互溶,熔化量少时可以以固溶形式存在. 超过铜的固溶量后则以独立的富铁相形式存在,使得焊缝靠钢侧球状铜区域由单一的 α-Cu 固溶体变为 α-Cu 和 ($\alpha+\varepsilon$) 双相组织. 随着钢的的溶入量增大,富铁相逐渐增多,晶粒尺寸也变大了,当铁的量进一步增加,而铜固溶铁的能力不足时,熔池冷却凝固过程中,球状富铁相来不及析出,故以球状铜内包含球状富铁相的形式存在于焊缝中,这是由于高温时溶解在铜溶液中的铁当温度下降时溶解度减小结晶析出造成的.

在形成液态球的过程中铁并没有与铜发生充分混合,但是由于铁、铜液态无限互溶,所以液态铁球在液态铜熔池内运动过程中,其中通过溶解、扩散的形式混入了一定量的铜. 而在随后的焊接冷却过程中,生成含有过饱和铜的 α-Fe 固溶体,由于焊接过程是个快速冷却的过程,因此溶解于其中的过饱和铜在富铁相结晶体过程中来不及排除.

3　结　　论

(1) 通过合理设置工艺可以得到较为理想的单面焊双面成形的焊接接头,焊缝表面无气孔、裂纹、未熔合等现象,焊缝熔合均匀,铜熔化量适宜,接头

抗拉强度可达 176 MPa，试样断裂于铜母材热影响区.

(2) 使用金相显微镜观察焊缝的显微组织，在焊缝区中心显微组织呈细胞群状，界面两侧的组织特征呈现显著的不同，焊缝与铜侧界面没有明显的熔合线，局部呈漩涡状，钢侧与焊缝连接处出现了明显的分界线.

(3) 通过分析各工艺参数对焊接质量的影响，当焊接电流为 65 A，焊接速度为 0.4 cm/s，离子气体流量为 0.7 L/min 时，能够获得质量较理想的接头.

参考文献:

[1] 巩水利. 高能束流加工技术的应用与发展 [J]. 航空制造技术，2009，20(14)：34－39.
Gong Shuili. Development and application of high energy beam processing technology [J]. The Technologies of Aerospace Manufacturing，2009，20(14)：34－39.

[2] 李亚江，王 娟，刘 鹏. 异种难焊材料的焊接及应用 [M]. 北京：化学工业出版社，2004.

[3] 雷玉成，郑惠锦. 工艺参数对焊接等离子弧的影响 [J]. 焊接学报，2001，22(6)：73－76.
Lei Yucheng，Zheng Huijin. The effect of parameters on plasma arc welding [J]. Transactions of the China Welding Institution，2001，22(6)：73－76.

[4] 黄春平，邢 丽，柯黎明，等. 紫铜与低碳钢厚板搅拌摩擦焊工艺分析 [J]. 焊接学报，2009，30(12)：37－40.
Huang Chunping，Xing Li，Ke Liming，*et al*. Technology of friction stir welding for copper and mild steel thick plate [J]. Transactions of the China Welding Institution，2009，30(12)：37－40.

[5] 邢 丽，李 磊，柯黎明，等. 低碳钢与紫铜搅拌摩擦焊接头显微组织分析 [J]. 焊接学报，2007，28(2)：17－20.
Xing Li，Li Lei，Ke Liming，*et al*. Microstructural investigation on friction stir welds of dissimilar metals between mild steel and copper [J]. Transactions of the China Welding Institution，2007，28(2)：17－20.

[6] 王宗杰. 熔焊方法及设备 [M]. 北京：机械工业出版社，2006.

作者简介： 程东海，男，1984 年出生，博士，讲师. 主要从事先进材料焊接方面的科研和教学工作. 发表论文 30 余篇. Email：chengdonghaicdh@yahoo.com.cn

coarse grain zone were investigated. The results illustrated that there were mainly four types of microstructure in coarse grain zone of high-strain pipeline steel X80, which includes polygonal ferrite(PF) and a small quantity of pearlite, granular bainite, bath bainite and bath martensite. The softening in coarse grain zone is an ubiquitous problem for high-strain pipeline steel X80. While the cooling rate after welding was between 15 ℃/s and 30 ℃/s, the coarse grain zone was mainly composed of bath bainite, which has the better microhardness, charpy toughness at room temperature and -10 ℃.

Key words: high-strain; X80 pipeline steel; coarse grain zone; microstructure; microhardness; toughness

Plasma arc welding of copper-steel dissimilar metals

CHENG Donghai, SHAO Jinghui, CHEN Yiping, HU Dean (Nanchang Hangkong University, Nanchang 330063, China). pp 97 - 100

Abstract: Experiment research on plasma arc welding of dissimilar metals between T2 copper and Q235 steel was carried out with LHM-200 plasma arc machine. A defect-free joint with good weld appearance was obtained. Microstructure of welded joint were analyzed by optical microscopy, and the effect rules of process parameters on mechanical properties of joint were analyzed. The results indicated that microstructure of the center of weld bead was like cell population shape. The microstructure characteristics of weld bead close with Cu-based metal was different with that close to Fe-based metal. The optical welding parameters were 65 A of weld current, 0.4 cm/s of welding speed, 0.7 L/min of plasma flow, and the tensile strength of welded joint reached 176 MPa with these parameters, and the fracture happened at the HAZ of copper side.

Key words: dissimilar metals of copper-steel; plasma arc welding; mechanical properties

Effect of amplitude on microstructures and representative element distribution in linear friction welded joint

JI Yajuan[1], LIU Yanbing[2], ZHANG Tiancang[1], ZHANG Chuanchen[1] (1. AVIC Beijing Aeronautical Manufacturing Technology Research Institute, Beijing 100024, China; 2. No. 94170 Unit of People's Liberation Army, Xi'an 710061, China). pp 101 - 104

Abstract: TC11 and TC17 titanium alloy usually used in aero engine blisk were welded with linear friction welding, the microstructures and element distribution were analyzed and tested by metallographic and electron probe, respectively. The temperature during the welding process was also measured. Results showed when the other parameters are constant, the width of TC17 thermal mechanical affected zone increases with the amplitude decreases, and microstructures of thermal mechanical affected zone at both sides are elongated along the stress direction and the nugget zone is composed of dynamic recrystallized grains. Cr distribution distance was farther when the amplitude at a higher value. The temperature measured results showed the maximum temperature can be up to 1 200 ℃ which exceeds the titanium beta transformation.

Key words: linear friction welding; titanium; microstructure; temperature

Quantitative analysis on interaction between corrosion and wear of NiCrBSiMo laser cladded coatings

SUN Lei, YUAN Jinping, ZHAO Junjun, LIANG Zhijie (Faculty of Remanufacturing Engineering, Academy of Armored Forces Engineering, Beijing 100072, China). pp 105 - 108

Abstract: Five kinds of Ni-based alloy coatings with 0, 2.5%, 5%, 7.5% and 10% Mo were prepared on the surface of 45CrNi steel plates by using CO_2 laser cladding equipment. The weight losses of corrosive wear in 3.5% NaCl solution of NiCrBSiMo laser cladded coatings were tested with a ball-on-disc wear tester. By means of tests and calculations, the weight loss of corrosion, wear and the components of interaction during corrosive wear tests were analyzed quantitatively. The results show that the total weight loss induced by corrosive wear is composed of the weight loss induced by simple wear and interaction. At the same time, the weight loss induced by interaction occupies about 24% ~56% in the total weight loss. Whereas, the weight loss induced by simple corrosion can be neglected. Moreover, the weight loss of coatings induced by wear under corrosive wear is 1.3 ~ 2.3 times compared to that of simple wear and the increased weight loss of wear induced by corrosion which occupies more than 99% in the total weight loss induced by interaction. The weight loss of coatings induced by corrosion under corrosive wear is 1.4 ~ 2.7 times compared to that of corrosion in the pure condition and both of values are small.

Key words: laser cladding; corrosion and wear; interaction; quantitative analysis

Microstructure and fatigue crack growth behavior of electron beam welded joints for TC4-DT titanium alloy

TANG Zhenyun[1,3], MA Yingjie[2], MAO Zhiyong[3], LEI Jiafeng[2], LIU Yuyin[2], LI Jinwei[3] (1. College of Mechanical Engineering and Applied Electronics Technology, Beijing University of Technology, Beijing 100124, China; 2. Institute of Metal Research, Chinese Academy of Sciences, Shenyang 110016, China; 3. Key Lab for High Density Beam Manufacture Technology, Beijing Aeronautic Manufacturing Technology Research Institute, Beijing 100024, China). pp 109 - 112

Abstract: The microstructure of electron beam welded joints of TC4-DT titanium alloy was analyzed by optical microscope, and the microstructure characteristics of different position in the joint were also analyzed. The crack propagation path and its growth rate were investigated on the joint samples, which the initial crack appeared at different location of the welded joints. Based on the microstructure characteristics of the welded joints, the influences of the weld microstructure on fatigue crack growth behavior were discussed. The results show that there are differences in the microstructure for electron beam welded joint along penetration depth. The fatigue crack propagation resistances of the weld fusion zone and heat affected zone were higher than that of the base metal, and the crack propagation path of the joints gradually tended to base metal zone. The influence of the crack propagation path offsets on crack growth rate was finally discussed in the paper.

Key words: TC4-DT titanium alloy; electron beam welding; weld microstructure; fatigue crack growth